

Multiphonon resonant Raman scattering in high-manganese-concentration $\text{Cd}_{1-x}\text{Mn}_x\text{Te}$ films

W. J. Keeler and H. Huang

Department of Physics, Lakehead University, Thunder Bay, Ontario, Canada P7B 5E1

J. J. Dubowski

Division of Physics, National Research Council of Canada, Ottawa, Canada K1A 0R6

(Received 28 June 1990)

We have measured resonant Raman scattering and photoluminescence (PL) from $\text{Cd}_{1-x}\text{Mn}_x\text{Te}$ (111) films deposited on (111)-oriented GaAs substrates. Film thickness varied from 0.6 to 1.8 μm and manganese concentrations x varied from 0.44 to 0.70 in the seven samples produced for this study using pulsed laser evaporation and epitaxy. Raman scattering shows that the films are of high quality throughout the composition range. The "CdTe-like" and "MnTe-like" LO-phonon modes appear in combinations up to the eighth order at 13 K under outgoing resonance conditions near the E_0 gap PL emission peak. Using Raman LO-phonon energy-composition relations reported in the literature for bulk $\text{Cd}_{1-x}\text{Mn}_x\text{Te}$, we have estimated the film Mn compositions and found them to be in close agreement with values obtained using energy-dispersive x-ray analysis (EDAX). The PL peak energy was also used to estimate the manganese composition. The best agreement with the Raman and EDAX determinations results when the PL emission is interpreted as being due to a neutral acceptor-bound magnetic polaron instead of an exciton process.

The bulk $\text{Cd}_{1-x}\text{Mn}_x\text{Te}$ (CMT) semiconductor alloy system has been studied extensively because of the wide tunability of its gap (1.58 to 2.30 eV as x ranges from 0 to 0.7) and the many novel properties and potential applications it might have in the visible region. The unfilled $3d$ shell in the Mn produces localized magnetic moments which interact with the conduction- and valence-band electrons, resulting in very strong magnetic and magneto-optic effects.¹⁻⁴ For several years high-quality thin films, epilayers, and quantum-well structures have been deposited on commercially available substrates. While much of this work has been accomplished using molecular-beam epitaxy (MBE),⁵⁻⁷ in anticipation of the need to reduce fabrication costs, films have been deposited using metal-organic chemical vapor deposition^{8,9} (MOCVD) ionized-cluster-beam techniques¹⁰ and pulsed laser evaporation and epitaxy (PLEE).¹¹ The film growth results reported so far have been mainly for low Mn composition samples ($x < 0.35$). However, recently, one of us¹² has reported PLEE-grown alloys with Mn concentrations approaching the zinc-blende structural limit of $x = 0.7$. In this paper we further investigate the properties of these higher-range-Mn-concentration samples using Raman and photoluminescence (PL) techniques.

To date most of the Raman spectra from bulk and film CdTe and $\text{Cd}_{1-x}\text{Mn}_x\text{Te}$ have shown only low overtone numbers (order $m = 1-3$). However, LO overtones up to $m = 4$ have been reported in MOCVD-grown CMT samples⁸ and $m = 6$ overtones have been reported by Feng and co-workers¹³ for PLEE-grown CdTe under outgoing resonance conditions near the $E_0 + \Delta_0$ gap. Here we report Raman results with LO-phonon overtones up to $m = 8$ and related PL for CMT epilayer films grown on GaAs (111) using PLEE. The overtones originate as outgoing resonant Raman scattering at what is believed to be

acceptor-related photoluminescence just below the fundamental gap E_0 .

The $\text{Cd}_{1-x}\text{Mn}_x\text{Te}$ (111) alloy films were grown on Si-doped GaAs (111) substrates using the PLEE method at the National Research Council of Canada. A high-vacuum deposition system employing dual pulsed lasers [excimer and Nd:YAG (Nd-doped yttrium aluminum garnet)] was used to grow the films. Vapors produced by simultaneous pulse evaporation from two targets were deposited epitaxially on a heated GaAs substrate. A XeCl excimer laser operating at 0.308 μm and triggered at up to 80 Hz vaporized $\text{Cd}_{0.44}\text{Mn}_{0.56}\text{Te}$ targets, while a Nd:YAG laser triggered between 0.5 and 5 kHz was used to generate additional Cd flux. The small laser spot size at the target pellet and the near ambient temperature of the unablated target bulk contribute to the production of very clean films. Due to the pulsed character of the evaporation process, film thickness can be controlled to the submonolayer level. Under optimized film growth conditions (excess Cd flux and substrate temperatures in the 210–290 °C range) *in situ* reflection high-energy electron diffraction showed sharp (111) patterns and scanning electron microscopy revealed in most cases a featureless surface morphology. Energy-dispersive x-ray analysis (EDAX) was used to obtain average composition readings for each film. The analyzed area was about $50 \times 50 \mu\text{m}^2$ and the x values are listed in Table I. No clustering of the Mn or Te was apparent in the seven samples prepared for this study. Further details of the sample preparation are given elsewhere.¹²

Raman and resonant Raman measurements were performed in the 90° backscattering geometry at Lakehead University. The samples were mounted on the cold finger of a closed-cycle helium refrigerator, which could be held at any temperature down to about 12 K. Temperature

TABLE I. Properties of PLEE $\text{Cd}_{1-x}\text{Mn}_x\text{Te}$ (111) layers grown on GaAs (111) substrates.

Sample	T_s ($^{\circ}\text{C}$)	d (μm)	EDAX	x	PL_{exc}	PL_{BMP}	Raman
CMT-1	210	0.8	0.70				0.70
CMT-2	250	0.6	0.51	0.48	0.54		0.54
CMT-3	270	1.4	0.50	0.44	0.51		0.51
CMT-4	290	1.1	0.51	0.43	0.50		0.50
CMT-5	270	0.9	0.56	0.49	0.56		0.56
CMT-6	270	1.2	0.54	0.51	0.57		0.58
CMT-7	290	1.8	0.45	0.36	0.42		0.44

measurement and control were accomplished using a Lakeshore Model DRC-91C controller with calibrated Si thermometer mounted next to the sample on the supporting brass finger. The Raman signal was excited with various lines of an Ar^+ -ion laser focused to a spot size of about 0.25 mm. The scattered light was analyzed using a Jobin-Yvon S-3000 triple spectrometer in the photon-counting mode, with slit settings yielding a resolution of $\sim 3 \text{ cm}^{-1}$. The detector was a thermoelectrically cooled Hamamatsu 934-02 photomultiplier.

Figure 1 shows the Raman spectrum for sample CMT-5 at 13 K. The excitation intensity was 50 mW at 488 nm. Phonon lines occur at multiples and combinations of the "CdTe-like" LO_1 and "MnTe-like" LO_2 phonon frequencies up to eighth order. Such high-order overtones are shown for the first time in CMT, and we take this as an indication of the high quality of the films. The peaks associated with the fifth overtones lie at the top of the PL emission and are reduced in intensity as compared to

those of the fourth and sixth overtones. This is in contrast to the behavior seen in CdTe overtone enhancement where the strongest effect occurs at the PL emission maximum.

Figure 2 shows photoluminescence and Raman lines for the 1.4- μm -thick sample CMT-3 excited with the 488-nm laser line. The photoluminescence was taken with 10 mW of input power while the Raman excitation intensity was 50 mW. The broad, intense emission centered at 2.0 eV is identified as the Mn^{2+} luminescence band which has an excitation threshold of 2.15 eV.^{14,15} The peak at 2.28 eV (and a similar Mn concentration-dependent peak in the other samples) is either a neutral acceptor-bound exciton luminescence (A^0, X) or an acceptor-bound magnetic polaron (BMP) peak (e, A^0), as discussed in detail by Bugajski *et al.*¹⁶ They showed that in p -type doped bulk samples, as x is increased from 0 to 0.3, the neutral donor-bound exciton (D^0, X), neutral acceptor-bound exciton (A^0, X) acceptor-bound magnetic

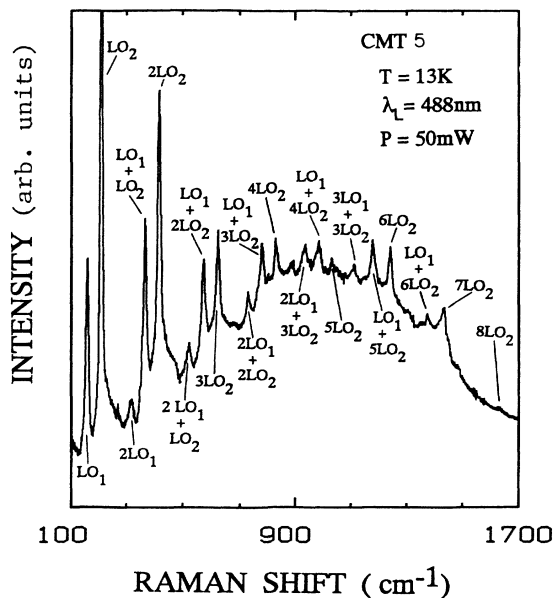


FIG. 1. Raman spectrum of PLEE-grown $\text{Cd}_{0.44}\text{Mn}_{0.56}\text{Te}$ (111) film (0.9 μm thick) on GaAs (111) measured at 13 K. Outgoing resonant enhancement occurs with the PL emission near the E_0 gap.

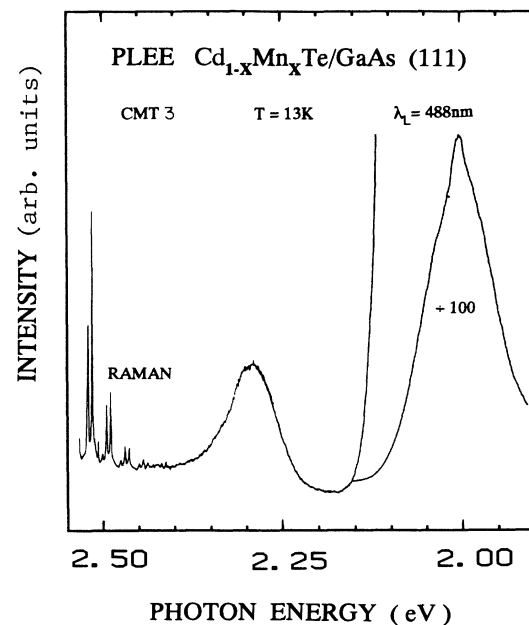


FIG. 2. Photoluminescence and Raman lines for sample CMT-3 with Mn composition $x=0.51$ and a thickness of 1.4 μm . The PL peak at 2.30 eV appears to be a bound magnetic polaron emission. The 2.0-eV peak is the Mn^{2+} luminescence.

polaron intensities change rapidly with composition. As x increases, the exciton emissions rapidly weaken and broaden in energy, while the BMP emission intensity grows. The manganese fraction in our samples lies between $0.44 \leq x \leq 0.70$. At such high concentrations the (A^0, X) and (e, A^0) emissions are the most likely candidates for the luminescence. If the peak is due to exciton emission, its location would be within a few meV of the fundamental gap E_0 . The low-temperature relation for the free exciton energy versus composition from Ref. 9 for $T=2$ K (and to a good approximation $T=13$ K) is (in eV)

$$E_0(x) = 1.595 + 1.52(x) . \quad (1)$$

Bugajski and co-workers showed that the bound magnetic polaron energy saturates at ~ 110 meV below the conduction-band edge for $x \geq 0.25$. Thus, if the PL peak is due to a BMP emission, to obtain a composition estimate from it an offset of ~ 110 meV should be added to the peak energy before using Eq. (1). Under this assumption, values of composition x for six samples are given in Table I. The column labeled PL_{BMP} is calculated assuming the luminescence is due to a BMP, the column labeled PL_{exc} assumes that the emission is excitonic and offset below the gap by ~ 15 meV. No estimate is given for sample CMT-1 because at $x=0.70$, the PL emission lies at slightly higher energy than the 457.9-nm line of the Ar^+ -ion laser. It appears that the PL_{BMP} estimates agree best with other methods for determining the Mn content.

Figure 3 shows two Raman spectra for sample CMT-4 for exciting lines of 488.0 and 514.5 nm. The signal intensity for the upper curve is twice as strong as that for

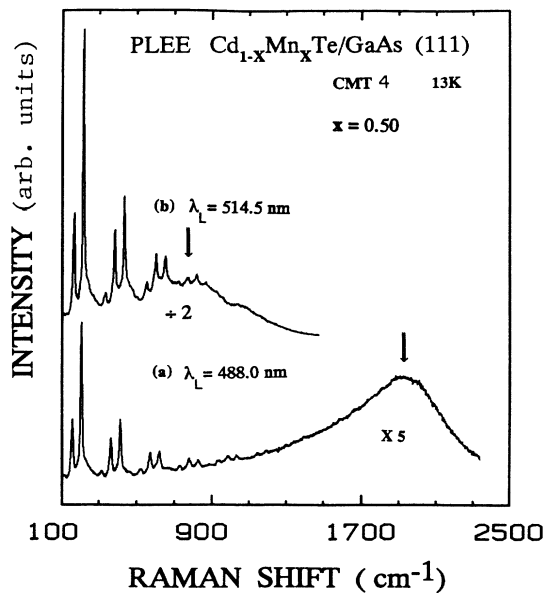


FIG. 3. Raman spectra for CMT-4 with excitation wavelengths of 488.0 and 514.5 nm. The arrows point to the same energy in each case. As increased resonance occurs in spectrum (b) the FWHM of the PL peak doubles and its intensity grows in proportion to the phonon intensities.

the lower, even though the excitation power is the same in both cases. Because of the scale reduction, there appears to be fewer overtones in the upper curve but both spectra show six. The arrows point to the same absolute energy in the two spectra and demonstrate that if the PL peak position is to be estimated accurately, it must be determined from nonresonant conditions.

In general, it was found that the resonance Raman enhancement increased as the incident photon energy approached the PL peak energy, but that the Raman intensity dropped rapidly when either the incoming or outgoing photon energy was less than the PL peak energy. This is illustrated in Fig. 4, which shows Raman spectra excited using the 488.0-nm Ar^+ -ion laser line for samples CMT-3, CMT-2, and CMT-6. Enhancement to the sixth or seventh overtone occurs when the outgoing photon energies straddle or lie to the high-energy side of the PL emission peak. The full width at half maximum (FWHM) PL peak width for resonant conditions averages 700–800 cm^{-1} in all samples, while the nonresonant peak width is 300–400 cm^{-1} . The former is at least twice as wide as the PL band associated with $E_0 + \Delta_0$ resonance enhancement in pure CdTe and may be additional evidence for interpreting the PL peak as being that of a bound magnetic polaron. It can also be seen that as the energy gap decreases with decreasing x the position of the PL peak moves towards lower energy and the enhancement weakens.

Venugopalan *et al.*¹⁷ have calibrated composition x for bulk alloy $Cd_{1-x}Mn_xTe$ samples against the “CdTe-like” and “MnTe-like” Raman LO and TO modes for room temperature and 80 K. We estimate the LO-mode energies by relations obtained from their graph.

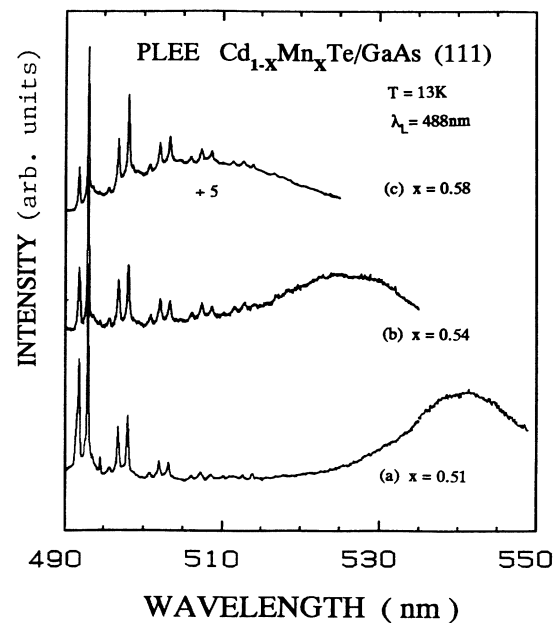


FIG. 4. Raman spectrum with PL peak for three samples with increasing Mn concentration and laser excitation at 2.541 eV. The PL-peak energy scales with x , even though the sample thicknesses vary by more than a factor of 2 (see Table I).

$E_{LO_1} = 173 - 26x$ for CeTe-like LO fundamental-mode energy, and $E_{LO_2} = 196 + 24x$ for the MnTe-like equivalent. The uncertainty in the intercepts is about 2 cm^{-1} at either end of the composition range. Positioning of the LO modes at 13 K should be about $1-2 \text{ cm}^{-1}$ higher in energy than their 80-K results, but differences between LO_1 and LO_2 energies would be essentially the same at the two temperatures. Using these assumptions, composition estimates for all the samples from fundamental LO peak locations are also given in Table I under the column titled Raman.

There is good agreement between the Raman estimate of composition, the EDAX estimate, and the PL_{BMP} estimate, considering that the uncertainty in the EDAX and Raman values are about ± 0.01 . Interpreting the PL emission as being due to a neutral acceptor-bound exciton (A^0, X) yields consistently low composition estimates. The agreement between the EDAX composition value (which samples the complete film thickness) and the less

penetrating Raman measurement suggests that the films are of uniform composition throughout. These spectra provide the basis for further theoretical analysis, particularly in regard to an understanding of the intensity distribution of the striking LO overtone structure. We hope to provide further insight into this in the near future.

In conclusion, observation of Raman modes from fourth order (nonresonant case) to eighth order under resonant conditions has been reported for the first time in high-concentration manganese CMT alloys. Good agreement between composition determinations using Raman, PL, and film averaging EDAX has been obtained. We believe that these results attest to the stability of the growth conditions and to the high quality of the PLEE-grown CMT/GaAs.

The work at Lakehead University was partially funded by a grant from the National Research Council of Canada.

-
- ¹R. R. Galazka, in *Physics of Semiconductors 1978*, edited by B. L. H. Wilson (The Institute of Physics, Bristol, 1979), p. 133.
- ²G. Bastard, C. Rigaux, Y. Guldner, J. Mycielski, and A. Mycielski, *J. Phys. (Paris)* **39**, 87 (1978).
- ³J. K. Furdyna, *J. Vac. Sci. Technol. A* **4**, 2002 (1986).
- ⁴E. K. Suh, D. U. Bartholomew, A. K. Ramdas, R. N. Bicknell, R. L. Harper, N. C. Giles, and J. F. Schetzina, *Phys. Rev. B* **36**, 9358 (1987).
- ⁵D. K. Blanks, R. N. Bicknell, N. C. Giles-Taylor, J. F. Schetzina, A. Petrou, and J. Warnock, *J. Vac. Sci. Technol. A* **4**, 2120 (1986).
- ⁶A. V. Nurmikko, R. L. Gunshor, and L. A. Kolodziejski, *IEEE J. Quantum Electron.* **QE-22**, 1785 (1986).
- ⁷S. Perkowitz, S. S. Yom, R. N. Bicknell, and J. F. Schetzina, *Appl. Phys. Lett.* **50**, 1001 (1987).
- ⁸Z. C. Feng, R. Sudharsanan, S. Perkowitz, A. Erbil, K. T. Pollard, and A. Rohatgi, *J. Appl. Phys.* **64**, 6861 (1988).
- ⁹Z. C. Feng, S. Perkowitz, and R. Sudharsanan, A. Erbil, K. T. Pollard, A. Rohatgi, J. L. Bradshaw, and W. J. Choyka, *J. Appl. Phys.* **66**, 1711 (1989).
- ¹⁰K. Nakamura, T. Koyanagi, K. Yamano, and K. Matsubara, *J. Appl. Phys.* **65**, 1381 (1989).
- ¹¹J. M. Wrobel and J. J. Dubowski, *Appl. Phys. Lett.* **55**, 469 (1989).
- ¹²J. J. Dubowski, *J. Cryst. Growth* **101**, 105 (1990).
- ¹³Z. C. Feng, S. Perkowitz, J. M. Wrobel, and J. J. Dubowski, *Phys. Rev. B* **39**, 12997 (1989).
- ¹⁴M. M. Moriwaki, R. Y. Tao, R. R. Galazka, W. M. Becker, and J. W. Richardson, in *Proceedings of the Sixteenth International Conference on the Physics of Semiconductors, Montpellier, France, 1987* [*Physica (Utrecht)* B+C **117-118**, 467 (1983)].
- ¹⁵V. F. Agekyan, Yu. V. Rud, and R. Schwabe, *Fiz. Tverd. Tela (Leningrad)* **29**, 1685 (1987) [*Sov. Phys.—Solid State* **29**, 970 (1987)].
- ¹⁶M. Bugajski, P. Becla, P. A. Wolff, D. Heiman, and L. Ram-Mohan, *Phys. Rev. B* **38**, 10512 (1988).
- ¹⁷S. Venugopalan, A. Petrou, R. R. Galazka, A. K. Ramdas, and S. Rodriguez, *Phys. Rev. B* **25**, 2681 (1982).